Geomechanics and Engineering, *Vol. 35, No. 5 (2023) 487-497*
https://doi.org/10.12989/gae.2023.35.5.487

Full-scale TBM excavation tests for rock-like materials with different uniaxial compressive strength

Gi-Jun Lee[1], Hee-Hwan Ryu*[2], Gye-Chun Cho[3] and Tae-Hyuk Kwon[3]

[1]*Korea Atomic Energy Research Institute, 111, Daedeok-daero 989beon-gil, Yuseong gu, Daejeon, Republic of Korea*
[2]*Korea Electric Power Research Institute (KEPRI), Daejeon, 34056, Republic of Korea*
[3]*Department of Civil and Environmental Engineering, Korea Advanced Institute of Science and Technology (KAIST), Daejeon, 34141, Republic of Korea*

(*Received September 26, 2023, Revised November 13, 2023, Accepted November 14, 2023*)

Abstract. Penetration rate (*PR*) and penetration depth (*Pe*) are crucial parameters for estimating the cost and time required in tunnel construction using tunnel boring machines (TBMs). This study focuses on investigating the impact of rock strength on *PR* and *Pe* through full-scale experiments. By conducting controlled tests on rock-like specimens, the study aims to understand the contributions of various ground parameters and machine-operating conditions to TBM excavation performance. An earth pressure balanced (EPB) TBM with a sectional diameter of 3.54 m was utilized in the experiments. The TBM excavated rock-like specimens with varying uniaxial compressive strength (UCS), while the thrust and cutterhead rotational speed were controlled. The results highlight the significance of the interplay between thrust, cutterhead speed, and rock strength (UCS) in determining *Pe*. In high UCS conditions exceeding 70 MPa, thrust plays a vital role in enhancing *Pe* as hard rock requires a greater thrust force for excavation. Conversely, in medium-to-low UCS conditions less than 50 MPa, thrust has a weak relationship with *Pe*, and *Pe* becomes directly proportional to the cutterhead rotational speed. Furthermore, a strong correlation was observed between *Pe* and cutterhead torque with a determination coefficient of 0.84. Based on these findings, a predictive model for *Pe* is proposed, incorporating thrust, TBM diameter, number of disc cutters, and UCS. This model offers a practical tool for estimating *Pe* in different excavation scenarios. The study presents unprecedented full-scale TBM excavation results, with well-controlled experiments, shedding light on the interplay between rock strength, TBM operational variables, and excavation performance. These insights are valuable for optimizing TBM excavation in grounds with varying strengths and operational conditions.

Keywords: penetration depth; rock-like material; TBM; tunnelling; UCS

1. Introduction

The penetration rate (*PR*) and penetration depth (*Pe*) of a Tunnel Boring Machine (TBM) are crucial parameters used to estimate the cost and time required for tunnel construction. These parameters effectively measure the TBM's excavation performance. Factors such as ground conditions, machine specifications, and the operator's judgment significantly impact the TBM penetration rate (Torabi *et al.* 2013, Hassanpour *et al.* 2010). Previous studies have developed models to predict the TBM penetration rate based on field data (e.g., Yagiz 2008, Hamidi *et al.* 2010, Delisio *et al.* 2013, Salimi *et al.* 2016, Naghadehi and Ramezanzadeh 2017, Jamshidi 2018). In these studies, the unconfined compressive strength (UCS) is commonly used as the primary strength property to assess the mechanical characteristics of rock masses (Lakshminarayana *et al.* 2021, Naithani *et al.* 2022, Liu *et al.* 2022, Lawal *et al.* 2023, Park 2023, Yoon *et al.* 2023, Zhang *et al.* 2023) due to its abundant data availability, accessibility, and simplicity. However, other properties like brittleness and joint characteristics can also influence TBM excavation performance (Yagiz 2008, Mansouri and Moomiv 2010, Delisio and Zhao 2014, Paltrinieri *et al.* 2016). Nonetheless, field excavation results are often influenced by multiple variables and factors, which pose challenges for analysis.

On the other hand, laboratory disc cutter tests allow for the examination of cutting depth and penetration depth, but these tests typically involve single or dual disc cutters, failing to consider the complete set of discs on a cutterhead. This limitation hampers our understanding of the interactions between disc cutters.

To address these issues, this study investigates the effects of ground and operating conditions on TBM excavation performance, specifically focusing on penetration depth (*Pe*), through a full-scale TBM excavation test (Lee *et al.* 2019a). This testing method enables a comparison of the contributions of various ground parameters and machine-operating conditions to the excavation performance using well-controlled, and sometimes identical, specimens. A series of full-scale tests was conducted, varying the unconfined compressive strength (UCS) of synthesized rock-like mortar and concrete specimens, as well as adjusting the thrust force and cutterhead rotational speed. The interactions among these

*Corresponding author, Ph.D.
E-mail: hhryu82@kepco.co.kr

ISSN: 2005-307X (Print), 2092-6219 (Online)

parameters are analyzed based on the test results and existing literature data, leading to the development of a prediction model for penetration depth.

Therefore, when taking into account the UCS range of 21-100 MPa for the rock substitute samples made with concrete and mortar, the experimental findings in this study enable us to predict excavation results in soft and hard rocks according to the presence or absence of joints.

2. Materials and methods: Full-scale TBM excavation test

2.1 EPB-TBM used

An earth pressure balanced shield TBM (EPB-TBM) with a cutterhead diameter of 3.54 m is used for this study, its detailed specification can be found in Table 1 (Lee *et al.* 2021). The TBM cutterhead is fitted with 26 cutters, the cutters have a diameter of 432 mm (17 inches) (Fig. 1). The TBM is composed of a cutterhead, a hood, and a tail part. The total length is approximately 8 m, and ~8.5 m with the screw conveyor. The total mass is ~126 metric tons. There is a bar welded on the TBM body to prevent rolling.

2.2 Preparation of rock-like concrete and mortar specimens

In order to investigate how the presence or absence of coarse components in the rock affects TBM excavation, concrete and mortar samples with similar strengths but different particle sizes were used as the synthesized rock specimens for full-scale TBM excavation tests, as shown in Table 2. In addition, the mortar and the concrete samples focusing on rock classification by UCS, ranging from soft rock to hard rock were made to investigate the penetration depth of the TBM in the rock by the thrust and rotational speed of the cutterhead. Three concrete specimens were prepared, which shows the unconfined compressive strength of 21, 50 (Lee *et al.* 2019a), and 70 MPa, respectively. Three mortar specimens were synthesized with the unconfined compressive strength of 21, 55 (Lee *et al.* 2019a), and 100 MPa, respectively.

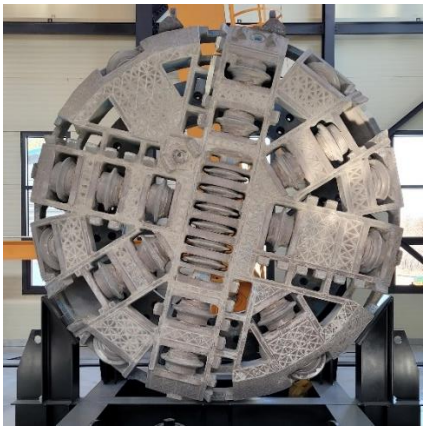

Fig. 1 Digital image of the cutterhead used for this study

Table 1 Specifications of the EPB-type TBM used in this study (Lee *et al.* 2021)

Part	Property	Specification
Cutter head	Cutting diameter	3622 mm
	Cutterhead diameter	3560 mm
	Maximum RPM	10 rev/min
	Torque	1380 kN·m
	Cutter size	430 mm (or 17 inches)
	Number of cutters	26
	Support type	Perimeter
	Opening ratio	15%
Cutter drive	Driving method	Hydraulic motor
	Power	630 kW
Shield body	Front shield diameter	3540 mm
	Overall length	7950 mm
Shield jack	Number of cylinders	12
	Maximum thrust per cylinder	1000 kN
	Stroke	1750 mm
Screw conveyor	Discharge capacity	Approximately 60.3 m^3/h
	Maximum RPM	20.7 rev/min
	Outer diameter	469 mm
	Inner diameter	415 mm
	Maximum Torque	13.23 kN·m

Table 2 Summary of the test conditions

Sample name	Material	UCS (MPa)	Thrust (kN)	Cutterhead speed (RPM)
CONC_LS	Concrete	21	2000	2.2, 4.4, 6.6, 7.9
			3000	2.2, 3.7, 6, 7.4
			4000	2.2, 3.1, 5, 5.8
CONC_MS		50	2000	1.4, 4.2, 5.3, 7.1
			3000	1.4, 3.9, 5.6, 8.3
			4000	2.2, 4.4, 6.3, 7.7
CONC_HS		70	2000	1.4, 4.4, 5.8, 7.3
			3000	1.4, 4.4, 5.8, 7.3
			4000	1.4, 4.3, 5.4, 6.8
			5000	4.3, 5.2, 7.7
MOR_LS	Mortar	21	2000	2.2, 3.3, 5.6, 6.9
			3000	2.1, 3, 6.5
			4000	2.2, 4.3, 6.2
MOR_MS		55	2000	1.4, 4.4, 5.9, 7.3
			3000	1.4, 4.1, 6.4, 8.3
			4000	1.4, 4.4, 5.8, 8
			5000	2.9, 5.3, 7.6
MOR_HS		100	2000	1.4, 4.4, 5.9, 7.3
			3000	1.4, 4.4, 5.8, 7.2
			4000	1.4, 4.2, 6.4, 7.3
			5000	1.4, 5.0, 5.4, 7.7

2.3 Test procedure

The test procedure involved several steps for the preparation and execution of the TBM excavation test, as follows. Firstly, the disassembly of the sample mold, support wall, and H-beam on the right side of the excavation direction was carried out (Lee *et al.* 2021). The front part of the TBM, consisting of the cutter head, hood

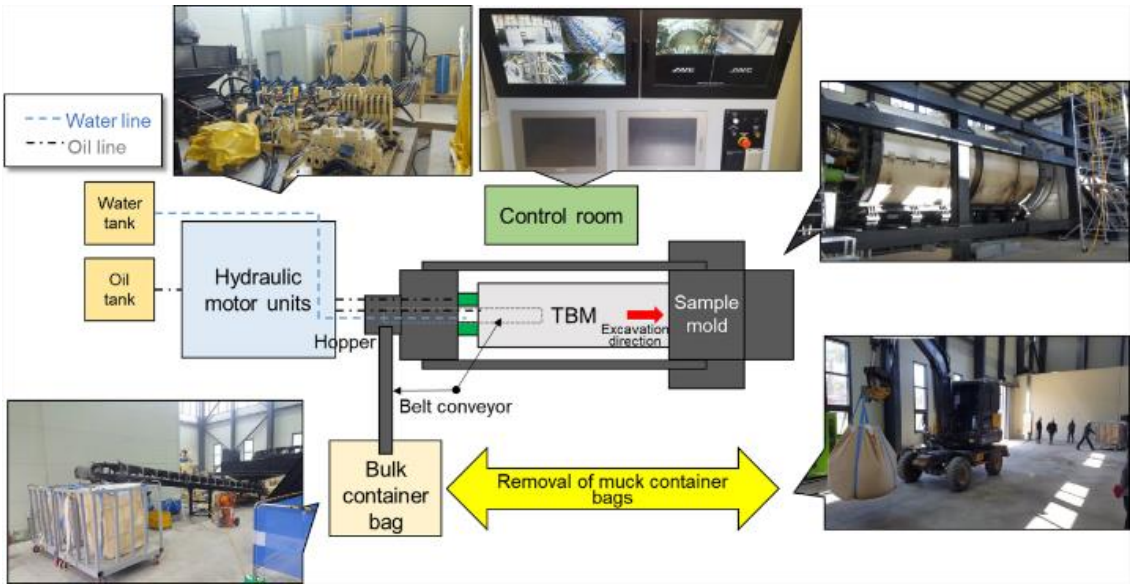

Fig. 2 Full-scale TBM excavation test process (Lee *et al.* 2021)

part, and tail part, was placed on the machine support. Additionally, a combined equipment setup was installed, including the support wall on the right side of the sample mold in the excavation direction, the H-beam to hold the sample mold abutment wall, and the propulsion abutment wall. Subsequently, the sample mold which is 5 m in width, 3.6 m in length, and 5 m in height, and is designed to endure the thrust and the pressure including impact by the failure of the samples was filled with concrete or mortar to simulate the rock mass. The mortar was produced by mixing water, cement, and sand, while the concrete was produced by mixing water, cement, fine aggregates, and coarse aggregates, and in some cases, additives such as plasticizer or slag were incorporated for manufacturability and strength enhancement. After a curing period of 28 days, unconfined compressive strength tests were performed on each specimen cylinder to ensure the attainment of the target strength. Once the curing was complete, the sample mold cover was installed.

To initiate the TBM excavation, the round plate at the inlet part of the soil box was replaced with a new entry part to accommodate the cutter head. A steel segment with a length of 2.25 meters was positioned inside the TBM, and a face frame was installed at the front side of the cylinders to facilitate the movement of the steel segment. The TBM was then positioned near the sample by pushing the cylinder into the entry part. The belt conveyor, screw conveyor, and cutter head were activated at the predetermined rotational speed (RPM). When the cutter head reached the target RPM, the excavation process commenced by applying thrust using the shield jacks at levels of 2000 kN and 3000 kN. The RPM of the cutter head was adjusted every 7-10 cm of penetration length, following a predetermined pattern. This process was repeated for higher thrust levels of 4000 kN and 5000 kN, with the RPM changing every 5-7 cm of penetration length. In order to exclude the influence of previous tests, as prior test conditions might affect subsequent ones, we conducted excavations of 7-10 cm or 5-7 cm for each condition to remove the initial data and analyzed the remaining data. The specific excavation conditions, including the cutter head RPM and thrust levels, are summarized in Table 2.

During the excavation process, as the TBM shield jacks advanced, the equipment cylinders pushed the segment to accommodate the shield jack stroke, thereby enabling the continuation of the excavation. Fig. 2 shows the configuration of the setup during the TBM excavation test (Lee *et al.* 2021).

3. TBM excavation test results and discussion

3.1 Penetration depth and rate with cutterhead speed and thrust

The TBM excavation test yielded valuable results regarding the penetration depth and rate. Concrete samples with unconfined compressive strength (UCS) values of 21 and 50 MPa, mortar samples with UCS values of 21 and 55 MPa, and a concrete sample with a UCS of 70 MPa were examined (Lee *et al.* 2019a). The analysis revealed that, with the exception of concrete and mortar with a UCS of 21 MPa, the penetration depth remained relatively constant across different cutterhead speeds (RPM) (Fig. 3). When the sample has a strength of 21 MPa, it experiences a substantial influence from a thrust of 2000 kN or more, irrespective of RPM. Consequently, the consistency of the RPM-dependent trend appears to be less pronounced compared to samples with higher strength. By comparing the TBM's operational conditions, it was possible to assess their influence on the penetration depth (*Pe*).

The penetration rate (*PR*) exhibited a linear relationship with RPM, regardless of the applied thrust and UCS values of the samples (Fig. 4). It is worth noting that the penetration depth generally corresponded to the thrust level (Fig. 5).

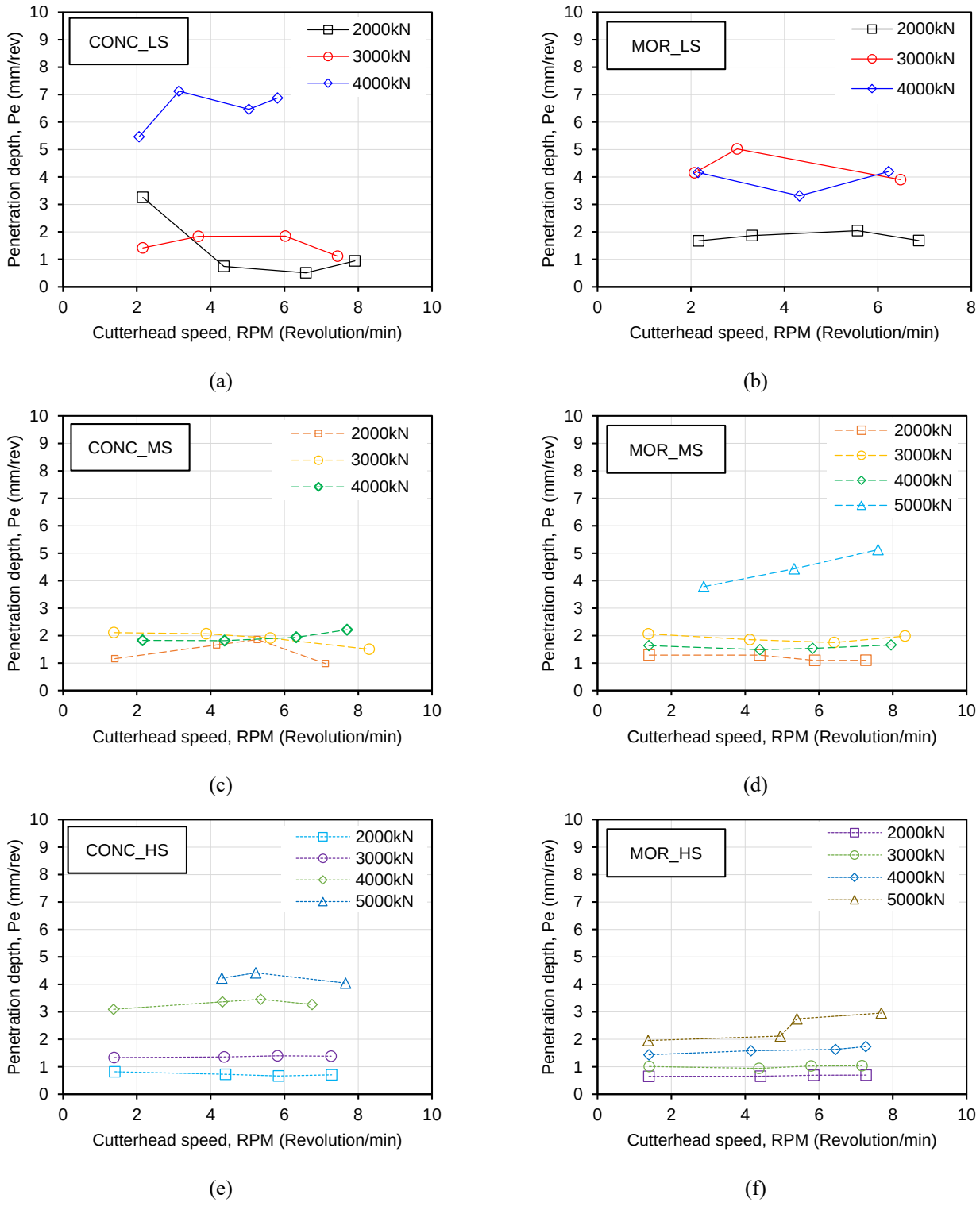

Fig. 3 Changes in penetration depth with cutterhead speed: (a, c, e) concrete samples, and (b, d, f) mortar samples

Furthermore, the obtained penetration depth results for the thrust per cutters fell within the range of results observed for rock samples (Fig. 5(b)) in previous studies (Gong *et al.* 2007, Ma *et al.* 2016). Notably, the penetration depth of the with RPM, regardless of the applied thrust and UCS values mortar sample with a UCS of 100 MPa closely resembled the results obtained from a laboratory cutting test on granite with a UCS of 105.6 MPa conducted by Ma *et al.* (2016).

In our study, the rotary cutting method (RCM) results in a larger cutting area compared to a linear cutting method (LCM), necessitating more energy. In addition, our study used the multi-cutters for the tests, but Ma *et al.* (2016) used a single cutter. Consequently, even though the strength

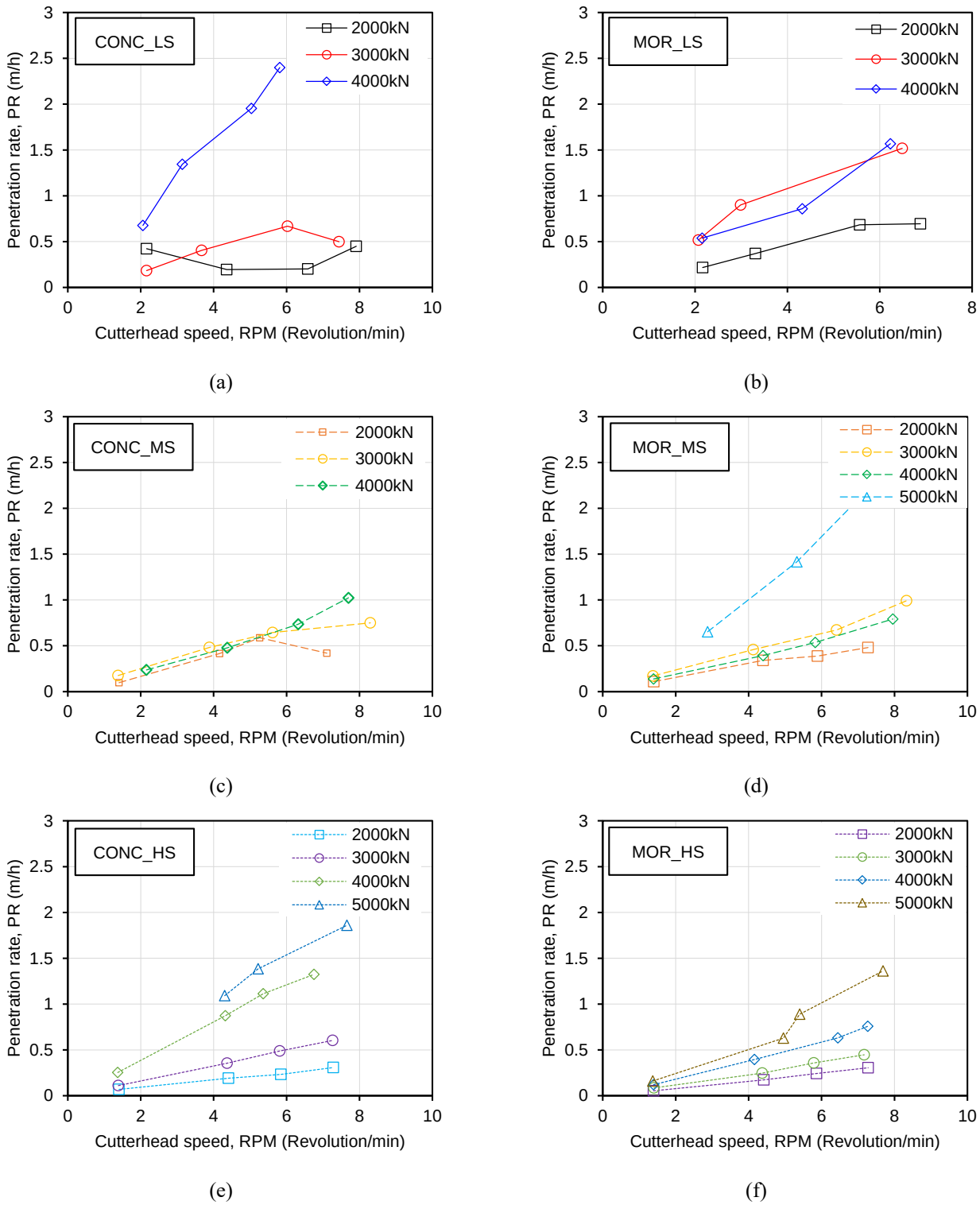

Fig. 4 Changes in penetration rate with cutterhead speed: (a), (c), (e) concrete samples, and (b), (d), (f) mortar samples

of the sample (MOR_HS) used in this test is 100 MPa, which is lower than sample's strength of 108 MPa from Ma *et al.* (2016), the observed penetration depth results closely resemble those obtained through the LCM test from Ma *et al.* (2016) by the differences in the method and the number of the used cutter.

However, when comparing the slope of the penetration depth with thrust per cutters reported by Gong *et al.* (2007), it was observed that their results exhibited a steeper and higher slope despite utilizing a sample with a higher UCS compared to the test samples. This discrepancy can be attributed to the differing characteristics of the samples. The homogeneous nature of the test samples, without any joints or discontinuities, contrasted with the sample from Gong *et al.* (2007) that contained joints, suggesting a relatively less homogeneous rock condition. Thus, it is evident that joints

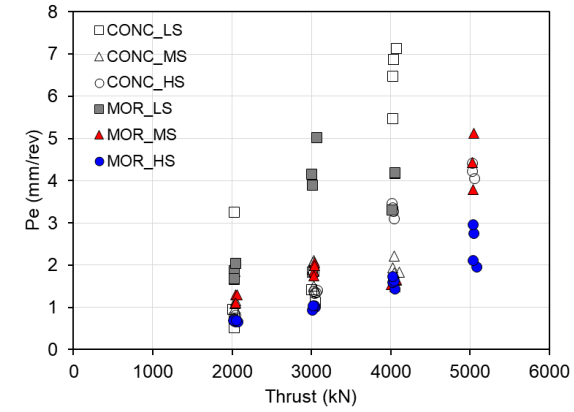

(a)

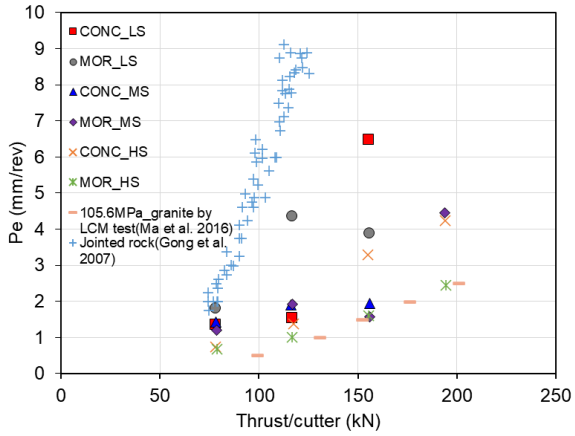

(b)

Fig. 5 Penetration depth with (a) thrust and (b) thrust per cutter

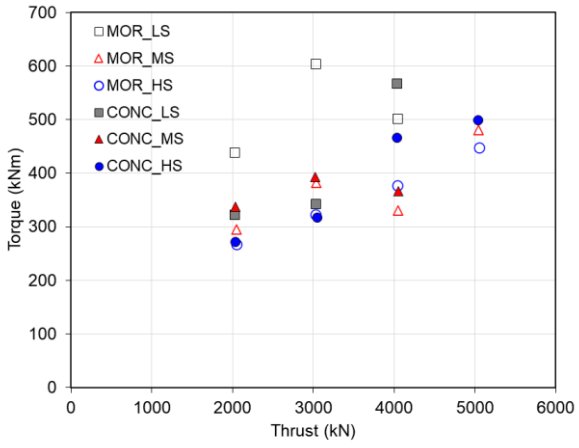

Fig. 6 Cutterhead torque with thrust for mortar and concrete samples

play a significant role as ground factors, exerting a substantial influence on TBM excavation outcomes. Fig. 5(b) shows the range of sample conditions considered, ranging from granite with a UCS of 105.6 MPa to jointed rock.

These results provide significant insights into the correlation between cutterhead speed, thrust, and penetration depth in TBM excavation. The findings enhance our understanding of excavation performance and offer valuable guidance for optimizing TBM operations in different ground conditions. The results emphasize the importance of carefully analyzing and controlling cutterhead speed and thrust levels to achieve desired excavation outcomes.

3.2 Torque with thrust, cutterhead speed, and penetration depth

The analysis of torque involved assessing the relationship between maximum torque and maximum cutterhead pressure, as described by Eq. (1) in the study.

$$Torque\left(kN\cdot m\right)=\frac{1350\left(kN\cdot m\right)}{34.3\left(MPa\right)}\cdot cutterhead\ pressure\left(MPa\right) \quad (1)$$

When examining thrust levels of 2000 kN and 3000 kN, it was observed that the torque was lowest for both concrete and mortar samples with the highest respective UCS values (Fig. 6). This outcome can be attributed to the smaller penetration depth achieved by samples with relatively weaker strength under the same thrust. Analyzing the torque with respect to cutterhead speed (RPM), it was evident that lower torque occurred around 4 RPM for samples with UCS values ranging from 50 MPa to 100 MPa, except for the case of concrete with a UCS of 50 MPa under a thrust of 2000 kN (Fig. 7).

Torque is influenced by several factors, including frictional force, thrust, and rotational force exerted by the cutterhead. The effective rotational force is primarily determined by the frictional force opposing the rotational force. Higher thrust results in a longer *Pe*, which in turn increases the resistance to rotational force due to greater contact between the cutters and the sample (Fig. 8).

Consequently, higher thrust leads to reduced effective rotational force and lower RPM. Conversely, increasing RPM enhances the effective rotational force while decreasing the effective thrust, as the application point of the effective thrust shifts to the upper groove of the sample. Thus, the optimal operational conditions of the TBM may vary based on specific combinations of thrust and RPM.

Therefore, it is crucial to determine the appropriate conditions for each sample, thrust level, and RPM. Considering the concrete and mortar samples with UCS values of 50 MPa, 70 MPa, 55 MPa, and 100 MPa, it can be inferred that the most suitable RPM is approximately 4 RPM, where the torque is minimized, particularly for the mortar samples, when applying thrust levels of 2000 kN, 3000 kN, and 4000 kN. Furthermore, when comparing the torque values with respect to sample composition, a notable distinction was observed between concrete and mortar samples with similar UCS values of 50 MPa. The concrete sample exhibited higher torque compared to the mortar sample with a UCS of 55 MPa, despite the mortar sample having a considerably higher UCS than the concrete sample (Fig. 7). This distinction arises from the presence of coarse

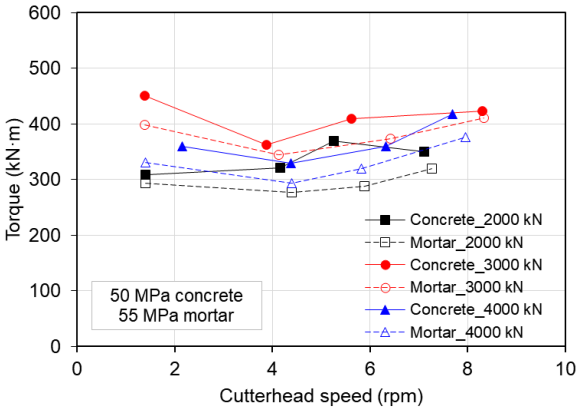

(a)

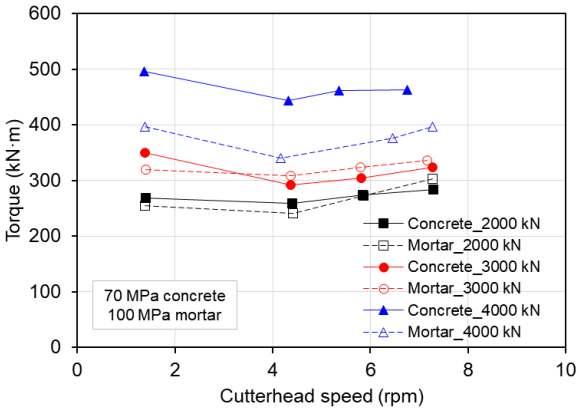

(b)

Fig. 7 Cutterhead torque with cutterhead speed: (a) for the samples with ~50 MPa UCS and (b) for the samples with 70 and 100 MPa UCSs

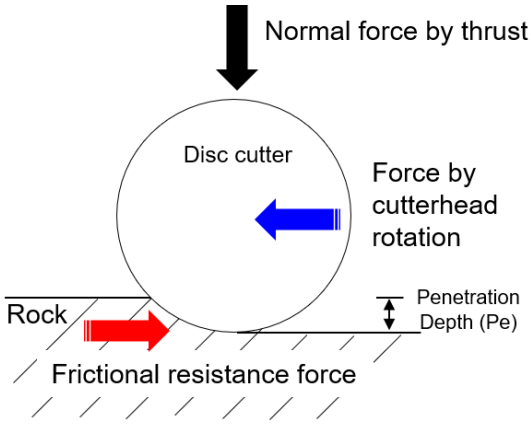

Fig. 8 Force applied to the disc cutter during TBM excavation

aggregates in concrete, which are larger than 20 mm. The presence of these coarse aggregates generates greater rotational resistance when the cutters engage with the sample, resulting in higher torque for the concrete sample compared to the torque recorded for the mortar sample.

By presenting these findings, the paper provides insights into the relationship between thrust, cutterhead speed, penetration depth, and torque in TBM excavation. These findings contribute to a deeper understanding of TBM performance and inform strategies for optimizing TBM operations under varying ground conditions.

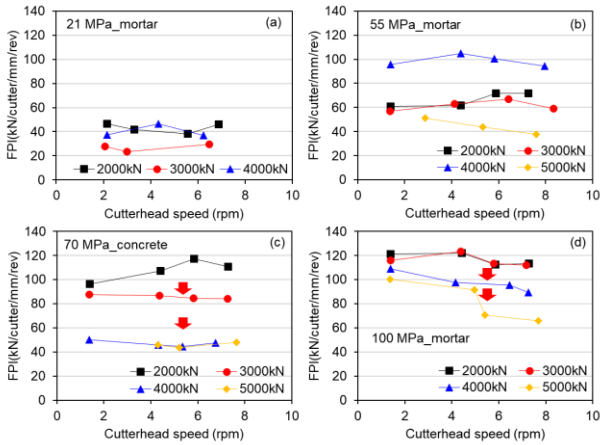

Fig. 9 Field penetration index with cutterhead speed: (a) for mortar with 21 MPa UCS, (b) for mortar with 55 MPa UCS, (c) for concrete with 70 MPa UCS, and (d) for mortar with 100 MPa UCS

4. Analysis

4.1 Analysis I: Field penetration index

The Field Penetration Index (*FPI*) serves as an efficiency index to evaluate TBM excavation performance and is expressed as follows

$$FPI\left[\frac{(kN \cdot rev)}{cutter \cdot mm}\right] = \frac{Th(kN) / N_C}{Pe(mm / rev)} \quad (2)$$

When examining the relationship between *FPI* and cutterhead speed (RPM) (Fig. 9), it became apparent that *FPI* remained relatively constant regardless of the cutterhead speed. This observation is attributed to the fact that *FPI* is primarily influenced by the *Pe*, which demonstrates consistency at a given thrust level. While no distinct relationship between *FPI* and thrust was observed for samples with unconfined compressive strength (UCS) values below 70 MPa, a notable trend emerged for samples with UCS values of 70 MPa and 100 MPa. Specifically, higher thrust resulted in lower *FPI* values.

This phenomenon can be attributed to the dominant role of thrust in causing failure of the excavated samples in the case of relatively high UCS values (Table 3). In the case of the sample with a UCS of 100 MPa, an increase in thrust from 2000 kN to 3000 kN yielded no significant change in *FPI*, while a noticeable change occurred when the thrust was further increased to 4000 kN. Therefore, for efficient excavation of the sample with a UCS of 100 MPa, a thrust greater than 4000 kN should be applied. Additionally, higher thrust levels corresponded to higher excavation efficiency. Similarly, a strong relationship between average *FPI* and thrust per cutter was observed for the concrete

Table 3 Comparison of the sample type to references

UCS of rock (MPa)	Sample type	Cutterhead speed effect	Thrust effect	Compare to references
21	Concrete	Penetration depth almost constant regardless of cutterhead speed (RPM)	A little effect with fracture by cutterhead rotation	Between jointed rock (Gong *et al.* 2007) and granite with UCS of 105.6 MPa (Ma *et al.* 2016)
21	Mortar			
50	Concrete			
55	Mortar			
70	Concrete		Thrust (Normal force) dominant	Granite with UCS of 105.6 MPa (Ma *et al.* 2016)
100	Mortar			

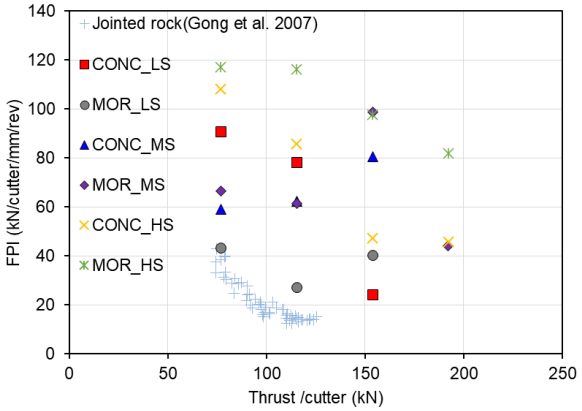

(a)

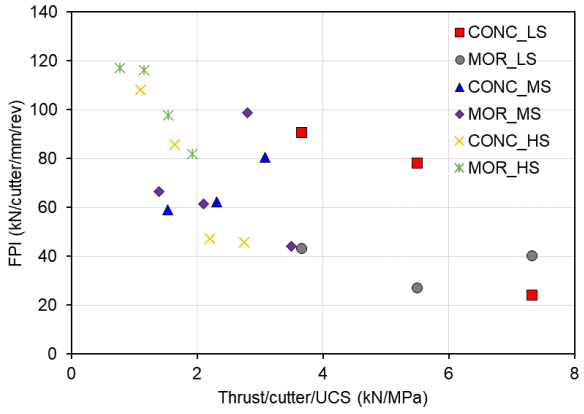

(b)

Fig. 10 Field penetration index (a) with thrust per cutter, and (b) with thrust per cutter normalized by UCS

sample with a UCS of 70 MPa and the mortar sample with a UCS of 100 MPa (Fig. 10(a)). In the case of jointed rock (Gong *et al*. 2007), characterized by strong rock strength, a clear correlation between *FPI* and thrust per cutter was evident. However, the presence of joints influenced the behavior of *Pe*, leading to increased *Pe* values in contrast to the observed trend in other sample cases. Notably, samples with relatively high UCS values exhibited *FPI* values distributed at higher levels compared to other samples (Fig. 10(b)). This finding indicates that stronger rock formations necessitate higher thrust levels for efficient excavation, thereby resulting in lower excavation efficiency.

By presenting these findings, the paper contributes to a comprehensive understanding of the relationship between *FPI*, cutterhead speed, thrust, and excavation efficiency in TBM operations. These insights are valuable for optimizing TBM performance in various ground conditions.

4.2 Relation between the penetration depth Pe and the cutterhead torque

In the relationship between *Pe* and torque (Fig. 11), the large torque caused a high *Pe* because the contact area between the cutter and the sample increases as *Pe* increases. As a result, the cutter receives more force when the cutterhead rotates. The relationship between *Pe* and torque exhibits a strong power relationship, with a determination coefficient of 0.84.

When the EPB-TBM with a diameter of 4.45 m was used to excavate slightly weathered rock mass, with an *RQD* of about 80 at the tunnel face, J_s was approximately 200 mm, and UCS was around 120 MPa in the field, the *Pe* obtained from the torque was larger than the test result (Gong *et al.* 2007).

The UCS of rock is affected by various factors such as sample size (Meikle and Holland 1965, Harrison and Hudson 2000), shape (Harrison and Hudson 2000), grain size (Brace 1961), moisture content (Colback and Wiid 1965), density, porosity (Price, 1960), and loading rate (Houpert 1970, Kobayashi 1970). Thus, UCS values under different rock sample conditions do not show an absolute relationship with excavation performance. Furthermore, there are joints and faults in the field that differ from the test conditions. Additionally, since the dip angle has a significant influence on the excavation rate, even if the UCS of the site sample is high, less energy may be required than the excavation test results in a homogeneous concrete or mortar mass. However, the trend of torque with *Pe* for values larger than 1 mm/rev was almost the same as the trend from the reference results (Gong *et al.* 2007). Therefore, considering the UCS and joints in the rock, it seems that the *Pe* can be indirectly predicted through the cutterhead torque. Furthermore, by comparing the rock mass strength obtained from ground investigation before TBM excavation with the TBM excavation results, it becomes possible to distinguish between an intact rock mass and one with numerous joints by analyzing the relationship between the *Pe* and the cutterhead torque.

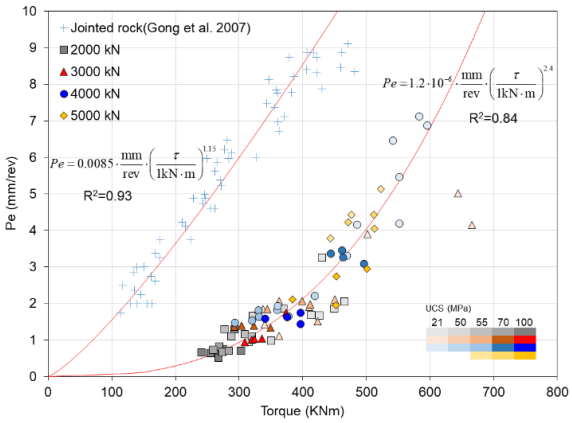

Fig. 11 Penetration depth with cutterhead torque

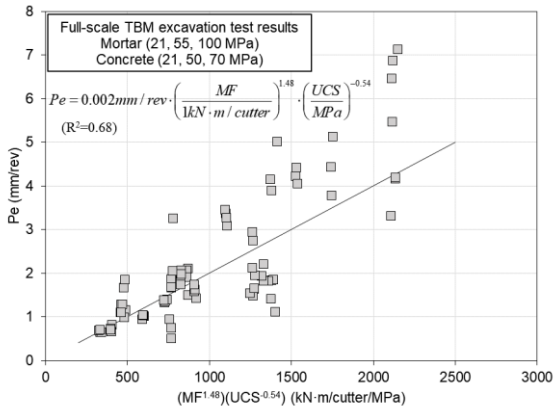

Fig. 12 Application of the simple model to predict Pe to the results of the full-scale TBM excavation tests

Consequently, the cutterhead torque can be adjusted to match the target excavation rate, providing the option to increase or reduce torque during TBM operation.

4.3 Prediction of Pe with UCS and the machine factors

The results of the tests were applied to the prediction model which was made by TBM excavation data with different UCS of rock and cutterhead diameter by Lee *et al.* (2019b) as follows

$$MF = \frac{Th \cdot D}{N} \tag{3}$$

$$Pe = \gamma \left[\frac{MF}{1kN \cdot m/cutter}\right]^{\alpha} \left[\frac{UCS}{1MPa}\right]^{\beta} \tag{4}$$

where, α, β and γ are the empirical parameters. For instance, α and β can be determined by finding the best fitting using the initial advance rate data in a TBM field, then the model with these parameters can be used to predict the *Pe* and *PR* for the rest of tunnel length. *MF* is a machine factor composed of thrust (*Th*), diameter of the cutterhead (*D*) and the number of cutters (*N*) (Lee *et al.* 2019b). The excavation parameters not only depend on the number of disc cutters but also depend on the layout of the disc cutters. In this study, however, we attempted to predict the penetration depth using the minimum factors that can be easily obtained, so that the layout of the disc cutters was not considered.

To verify the *Pe* prediction model, this model was applied to the results of the full-scale TBM excavation test. As a result, the prediction model predicted *Pe* with determination coefficient of 0.68 that is almost 0.7, which is as follows (Fig. 12).

$$Pe = 0.002 \text{ mm/rev} \cdot \left(\frac{MF}{1kN \cdot m/cutter}\right)^{1.48} \cdot \left(\frac{UCS}{MPa}\right)^{-0.54} \tag{5}$$

This model is constructed using TBM excavation data from rock masses of varying strengths. It produces predictive results with a coefficient of determination of around 0.7 for TBM excavation data related to concrete and mortar samples, which are rock-like materials. This indicates that, even though the concrete and the mortar are not actual rock masses, the behavior of TBM excavation into a rock mass based on its strength can be observed through the rock-like materials.

5. Conclusions

In conclusion, this study focused on investigating the impact of material strength and the presence of aggregates on TBM penetration depth and penetration rate. This was achieved through full-scale TBM excavation tests conducted on rock-like concrete and mortar specimens. The key findings of this research are as follows:

- Firstly, for media with high compressive strength, particularly those with a UCS exceeding 70 MPa, the normal force exerted by the discs driven by TBM thrust emerged as the primary factor influencing penetration depth and advance rate. Conversely, in medium-to-low strength media with a UCS less than 50 MPa, both the rotational force of discs driven by cutterhead torque and the normal force from thrust demonstrated significance in determining the penetration rate.
- Furthermore, the presence of coarse aggregates in the materials led to increased resistance to cutterhead rotation. Consequently, excavating concrete materials required higher cutterhead torque compared to excavating mortar materials. This observation holds relevance for various rock formations, including coarse-grained (conglomerates, breccia) and fine-grained (sandstones) sedimentary rocks.
- This study revealed that penetration depth (*Pe*) exhibited a direct relationship with cutterhead torque, with a power law effectively capturing their correlation. Leveraging the results of full-scale TBM excavation tests, we propose a predictive model for *Pe* that takes into account thrust, TBM diameter, number of disc cutters, and rock UCS.
- This study presents compelling and well-controlled experimental evidence linking TBM excavation performance to both thrust force and torque. These findings provide valuable insights for TBM excavation in grounds with varying strength characteristics, as demonstrated

through the comprehensive full-scale TBM tests conducted.

Overall, this study significantly contributes to our understanding of the factors influencing TBM performance and offers practical implications for optimizing excavation processes in different geological conditions. In addition, this study will be valuable for the development of a TBM excavation manual for rock, providing guidance on how to apply thrust and cutterhead rotational speed for targeted TBM excavation based on the UCS of the rock mass being excavated. It will also offer insights into how to operate the TBM for the remaining excavation based on data such as penetration depth, thrust, cutterhead rotational speed, and cutterhead torque obtained from the TBM excavation results.

Acknowledgments

This study was supported by a project (R23SA01) of Korea Electric Power Corporation Research Institute and by the Korea Electric Power Corporation (Grant R22XO05-11).

References

Brace, W.F. (1961), "Dependence of fracture strength of rock on grain size", *Proceedings of the 4th Symposium of Rock Mechanics*, University Park, Penn. USA.

Coalbak, P.S.B. and Wiid, B.L. (1965), "The Influence of moisture content on the compressive strength of rocks", *Proceedings of the 3rd Canadian Rock Mechanics Symposium*, Toronto, 65-83.

Delisio, A., Zhao, J. and Einstein, H.H. (2013), "Analysis and prediction of TBM performance in blocky rock conditions at the Lötschberg Base Tunnel", *Tunn. Undergr. Sp. Technol.*, **33**(1), 131-142. https://doi.org/10.1016/j.tust.2012.06.015.

Delisio, A. and Zhao, J. (2014), "A new model for TBM performance prediction in blocky rock conditions", *Tunn. Undergr. Sp. Technol.*, **43**, 440-452. https://doi.org/10.1016/j.tust.2014.06.004.

Gong, Q.M., Zhao, J. and Jiang, Y.S. (2007), "In situ TBM penetration tests and rock mass boreability analysis in hard rock tunnels", *Tunn. Undergr. Sp. Technol.*, **22**(3), 303-316. https://doi.org/10.1016/j.tust.2006.07.003.

Hassanpour, J., Rostami, J., Khamehchiyan, M., Bruland, A. and Tavakoli, H.R. (2010), "TBM performance analysis in pyroclastic rocks: a case history of Karaj water conveyance tunnel", *Rock Mech. Rock Eng.*, **43**(4), 427-445. https://doi.org/10.1007/s00603-009-0060-2.

Harrison, J.P. and Hudson, J.A. (2000), "Engineering Rock Mechanics", *Pergamon Press*, **2**(5), 499.

Hamidi, J.K., Shahriar, K., Rezai, B. and Rostami, J. (2010), "Performance prediction of hard rock TBM using Rock Mass Rating (RMR) system", *Tunn. Undergr. Sp. Technol.*, **25**(4), 333-345. https://doi.org/10.1016/j.tust.2010.01.008.

Houpert, R. (1970), "The uniaxial compressive strength of rocks", *Proceedings of the 2nd Congress of International Society of Rock Mechanics*, Belgrade.

Jamshidi, A. (2018), "Prediction of TBM penetration rate from brittleness indexes using multiple regression analysis", *Model. Earth Syst. Environ.*, **4**(1), 383-394. https://doi.org/10.1007/s40808-018-0432-2.

Kobayashi, R. (1970), "On mechanical behaviour of rocks under various loading rates", *Rock Mechanics in Japan*, **1**, 56-58.

Lakshminarayana, C.R., Tripathi, A.K. and Pal, S.K. (2021), "Experimental investigation on potential use of drilling parameters to quantify rock strength", *Int. J. Geo-Eng.*, **12**(1), 23. https://doi.org/10.1186/s40703-021-00152-5.

Lawal, A.I., Kim, M. and Kwon, S. (2023), "Soft computing based mathematical models for improved prediction of rock brittleness index", *Geomech. Eng.*, **33**(3), 279-289. https://doi.org/10.12989/gae.2023.33.3.279.

Lee, G.J., Kwon, T.H., Cho, G.C. and Kim, K.Y. (2019a), "Preliminary Result on Full-Scale TBM Excavation Tests", *Proceedings of the 32nd KKHTCNN Symposium on Civil Engineering*, October 24-26, 2019, Daejeon, Korea.

Lee, G.J., Kwon, T.H., Ryu, H.H., Kim, K.Y. and Oh, T.M. (2019b). "Effect of machine factors of tunnel boring machines on penetration rates in rocks", *Proceedings of the World Tunnel Congress, WTC 2019 and the 45th General Assembly of the International Tunnelling and Underground Space Association*, ITA-AITES 2019, CRC Press/Balkema.

Lee, G.J., Ryu, H.H., Kwon, T.H., Cho, G.C., Kim, K.Y. and Hong, S. (2021), "A newly developed state-of-the-art full-scale excavation testing apparatus for Tunnel Boring Machine (TBM)", *KSCE J. Civil Eng.*, **25**(12), 4856-4867. https://doi.org/10.1007/s12205-021-2347-0.

Liu, X., Zheng, Y., Hao, Q., Zhao, R., Xue, Y. and Zhang, Z. (2022), "Dynamic failure features and brittleness evaluation of coal under different confining pressure", *Geomech. Eng.*, **30**(5), 401-411. https://doi.org/10.12989/gae.2022.30.5.401.

Mansouri, M. and Moomiv, H. (2010), "Influence of rock mass properties on TBM penetration rate in Karaj-Tehran water conveyance tunnel", *J. Geol. Min. Res.*, **2**(5), 114-121. https://doi.org/10.5897/JGMR.9000039.

Ma, H., Gong, Q., Wang, J., Yin, L. and Zhao, X. (2016), "Study on the influence of confining stress on TBM performance in granite rock by linear cutting test", *Tunn. Undergr. Space Technol.*, **57**, 145-150. https://doi.org/10.1016/j.tust.2016.02.020.

Meikle, P.G. and Holland, C.T. (1965), "The effect of friction on the strength of model coal pillar", *Trans. Soc. Min. Eng. AIME*, **232**(4), 322-327.

Naghadehi, M.Z. and Ramezanzadeh, A. (2017), "Models for estimation of TBM performance in granitic and mica gneiss hard rocks in a hydropower tunnel", *Bull. Eng. Geol. Environ.*, **76**(4), 1627-1641. https://doi.org/10.1007/s10064-016-0950-y.

Naithani, A.K., Jain, P., Singh, L.G. and Rawat, D.S. (2022), "Engineering geological characteristics of the underground surge pool cavern: a case study, India", *Int. J. Geo-Eng.*, **13**(1), 7. https://doi.org/10.1186/s40703-022-00172-9.

Paltrinieri, E., Sandrone, F. and Zhao, J. (2016), "Analysis and estimation of gripper TBM performances in highly fractured and faulted rocks", *Tunn. Undergr. Sp. Technol.*, **52**, 44-61. https://doi.org/10.1016/j.tust.2015.11.017.

Park, D. (2023), "Stability analysis of infinite rock slopes with varying disturbances based on the Hoek–Brown failure criterion", *Geomech. Eng.* **33**(1), 53-63. https://doi.org/10.12989/gae.2023.33.1.053.

Price, N.J. (1960), "The compressive strength of coal measures rock", *Colliery Engineering*, **37**, 283-292.

Salimi, A., Rostami, J., Moormann, C. and Delisio, A. (2016), "Application of non-linear regression analysis and artificial intelligence algorithms for performance prediction of hard rock TBMs", *Tunn. Undergr. Sp. Technol.*, **58**(1), 236-246. https://doi.org/10.1016/j.tust.2016.05.009.

Torabi, S. R., Shirazi, H., Hajali, H. and Monjezi, M. (2013), "Study of the influence of geotechnical parameters on the TBM performance in Tehran–Shomal highway project using ANN and SPSS", *Arabian J. Geosci.*, **6**(4), 1215-1227. https://doi.org/10.1007/s12517-011-0415-3.

Yagiz, S. (2008), "Utilizing rock mass properties for predicting TBM performance in hard rock condition", *Tunn. Undergr. Sp. Technol.*, **23**(3), 326-339. https://doi.org/10.1016/j.tust.2007.04.011.

Yoon, S., Jeong, H., Lee, H.L., Kim T., Hong, C.H. and Kim, J.S. (2023), "Evaluation of uniaxial compression and point load tests for compacted bentonites", *Acta Geotech.,* **18**, 4633-4644. https://doi.org/10.1007/s11440-023-01844-1.

Zhang, J., Deng, R., Zhong, Z., Wu, P. and Qi, S. (2023), "An Investigation on Stress States of the Cataclastic Rock Specimen under Confined Compression Based on Modified Thick-walled Cylinder Model", *KSCE J. Civil Eng.*, **27**, 4215-4227. https://doi.org/10.1007/s12205-023-0097-x.

IC